ARMY RESEARCH LABORATORY

Flame Structure Studies of Neat and NH_3-Doped $H_2/N_2O/Ar$ Flames by Laser-Induced Fluorescence, Mass Spectrometry, and Modeling

by R. C. Sausa
and D. T. Venizelos

ARL-TR-1858 December 1998

The findings in this report are not to be construed as an official Department of the Army position unless so designated by other authorized documents.

Citation of manufacturer's or trade names does not constitute an official endorsement or approval of the use thereof.

Destroy this report when it is no longer needed. Do not return it to the originator.

Army Research Laboratory
Aberdeen Proving Ground, MD 21005-5066

ARL-TR-1858 **December 1998**

Flame Structure Studies of Neat and NH_3-Doped $H_2/N_2O/Ar$ Flames by Laser-Induced Fluorescence, Mass Spectrometry, and Modeling

R. C. Sausa, D. T. Venizelos
Weapons and Materials Research Directorate, ARL

Abstract

A combined experimental and modeling study of neat and NH_3-doped (Φ=1), 30-Torr flames is reported. The major species concentrations are measured by molecular beam mass spectrometry (MB/MS), whereas the minor species OH, NH, and O-atom concentrations are measured by laser-induced fluorescence (LIF). The species NO is measured both by LIF and MB/MS, and O_2 by MB/MS. The flame temperatures are measured both by OH and NH LIF and by thin wire-thermometry. The flames are modeled with PREMIX using the temperature profiles and several detailed chemical mechanisms as input. The mechanisms include the ***GRI 2.11***, ***SSLA***, and their derivatives. The ***SSLA*** mechanism was developed previously in our laboratory from a critical literature review. Calculations using all the mechanisms predict fairly well the profiles of the major species for both neat and doped flames. However, both the ***SSLA*** and ***GRI 2.11*** calculations fail to predict the postflame O_2 concentration in the neat flame, the drop in the O_2 concentration with the addition of NH_3, and the NH_3 decay in the doped flame. Sensitivity analyses suggest refinements to the ***SSLA*** and ***GRI 2.11*** mechanisms. The experimental results are predicted rather well using a ***modified SSLA*** mechanism in which the $NH+NO=N_2O+H$ reaction rate is decreased and the $N_2O+M=N_2+O+M$ reaction rate and/or H_2O third body efficiency is increased to the limit of their uncertainty. Rate analyses performed on the modeled calculations reveal the reactions important to NO, O_2, NH, OH, and O-atom production and consumption and NH_3 consumption. These reactions are presented and discussed.

Acknowledgments

We thank Drs. W. Anderson, A. Kotlar, and R. Pastel of the U.S. Army Research Laboratory (ARL), Dr. D. Dayton of the National Renewable Energy Laboratory, and Prof. G. Singh of the University of Maryland Eastern Shore for their helpful discussions. We also thank Dr. W. Anderson for carefully reviewing this manuscript. This work was supported by the ARL Mission Program on Combustion and the Strategic Environmental Research and Development Program (ERDP) on cleanup (ARMY-713-94 and ARMY-729-94). Support from the National Research Council (NRC) ARL Post-Doctoral Fellowship Program (D. T. Venizelos), and the Productivity Capital Investment Program (R. C. Sausa) is gratefully acknowledged.

Table of Contents

List of Figures

List of Tables

1. Introduction

The H_2/N_2O flame system has received considerable attention in recent years because it is an appropriate analog for experimental and modeling efforts to study NO_x pollutant formation and nitramine propellant combustion [1–3]. Such a flame system can provide additional information on the fundamental reaction mechanisms relevant to the nitrogen chemistry in more complex combustion systems. Recently, the role of NH_3 in converting NO to final products was investigated in our laboratory using neat and NH_3-doped H_2/N_2O/Ar low-pressure flames (Φ~1.1) [4]. The profiles of several species, such as H_2, N_2O, NH_3, H_2O, N_2, and NO, in both neat and doped flames, were obtained with molecular beam mass spectrometry (MB/MS). The experimental profiles were compared to predicted profiles, generated with the one-dimensional, laminar flame, PREMIX computer code using a detailed chemical mechanism ***(SSLA)*** derived from a critical literature review [4]. The modeled profiles of the major species agreed very well with the experimental profiles for the neat flame and reasonably well for the doped flame. However, there were discrepancies between the experimental and predicted NO profiles. Specifically, the model predicted a decay of the NO profile in the postflame region for the doped flame, while the experimental profile exhibited a plateau. In addition, the model overpredicted the NH_3 mole fraction in the postflame region and that this overprediction was the primary cause of the predicted NO decay. Calculations indicated that refinements to the chemical mechanism used by the numerical model were necessary.

Such refinements require comparing not only the experimental and predicted profiles of major species but also comparing the profiles of intermediate species. Unfortunately, these measurements prove to be difficult with MB/MS for a $H_2/N_2O/NH_3$ system because of interference between isobaric species such as O and NH_2, or OH and NH_3. Also, the measurements of NH may be obscured by the interference from NH_2 and NH_3 because of ionization fragmentation effects.

Reported in this paper is a combined experimental and modeling study of neat and NH_3-doped H_2/N_2O flames. The current work extends the previous study in our laboratory by introducing additional measurements of the O, OH, NH, and NO species using laser-induced fluorescence (LIF)

and O_2 using MB/MS. Flame temperatures are measured both by thin-wire thermometry and OH and NH LIF. The flames are modeled using the PREMIX flame code with the detailed ***SSLA*** [4] and ***GRI 2.11*** [5] mechanisms and their derivatives as input. Rate and sensitivity analyses reveal key reactions in the mechanisms, as well as the pathways for species production and consumption.

2. Experimental

The experimental apparatus consists of a variable-pressure burner equipped for MB/MS, LIF, and thin-wire thermometry. The details are discussed elsewhere [1, 2, 4]. Briefly, both the neat and NH_3-doped H_2/N_2O/Ar flames were supported on a 6-cm, stainless steel, McKenna flat burner mounted in a cylindrical vacuum chamber maintained at 30 Torr. The neat flame was stabilized by flowing a mixture of H_2, N_2O, and Ar at 1.41, 1.43, and 1.06 slm, respectively. This flame was then doped with 0.14 slm NH_3. The experimental apparatus was reconfigured for the present study so that the LIF and thermocouple flame measurements were performed at the same point and at the center of the burner directly beneath the MB/MS probe. A comparison between the MB/MS and LIF concentration profiles of NO indicated that the MB/MS sampling takes place approximately 1.5 mm (five nozzle diameters) below the probe tip. Cattolica, Yoon, and Knuth [6] also observed a shift of five nozzle diameters when measuring the OH radical by both laser absorption spectroscopy and MB/MS in a stoichiometric CH_4/air flame [6]. The present experimental configuration allows for a more accurate measurement of the flame temperatures and species concentrations because the LIF and thermocouple measurements are recorded exactly where the MB/MS is sampling. All the MB/MS data are shifted ~1.5 mm toward the burner surface for direct comparison to the LIF and thermocouple data.

A 20-Hz, Nd-YAG (Quantel, YG581C) pumped dye laser (Lambda Physik, FL3002) with a BBO frequency-doubling crystal was used for the NO, OH, NH, and O-atom IF measurements. Pulse energies of 100–500 μJ with 5% shot-to-shot fluctuation and 10-ns duration were obtained after frequency doubling. The 2-mm diameter laser beam was focused with a 200-mm focal length lens for O-atom LIF and a 500-mm focal length lens for NO, OH, and NH LIF. A shorter focal length

lens was required for O-atom LIF because of the multiphoton nature of the excitation process. A plot of LIF signal as a function of laser energy showed a near quadratic dependence, suggesting two-photon excitation.

The excitation/detection schemes for profiling the aforementioned species involve the following: (1) excitation of NO $A^2\Sigma^+ - X^2\Pi$ (0,0) Q_1 (26.5) and R_2 (25.5) transitions at 225.37 [7] and 225.03 nm, respectively, with subsequent (0,1) emission detection at 236 nm; (2) two-photon excitation of the O $3p^3P \leftarrow 2p^3P$ transition near 226 nm with $3p^3P \rightarrow 3s^3S$ emission detection at 845 nm; (3) excitation of OH $A^2\Sigma^+ - X^2\Pi$ (1,0) R_1 (7.5) transition at 281.1 nm with (1,1) emission detection at 313 nm, and (4) excitation of the NH $A^3\Sigma^+ - X^3\Pi$ (1,0) R_2 (9) transition at 302.65 nm with (1,1) emission detection at 337 nm. The fluorescence was collected at an angle normal to the excitation laser beam and viewed with a photomultiplier tube (Hamamatsu R955) equipped with an appropriate 10-nm (fwhm) interference filter for O and OH detection or a 1/8-m wide-slit (~10 nm at fwhm) monochromator (Jarrell Ash) for NO and NH detection. The excitation transitions were carefully selected for their temperature insensitivity by using the following equation [8]:

$$J^2 + J - \left(\frac{k}{hcB_v}\right) T_a v = 0, \qquad (1)$$

where J is the rotational energy level, T_{av} is the average flame temperature, and k, h, c, and B_v the usual spectroscopic constants. Boltzmann calculations show that for a 5% change in a 2,000 K flame temperature the LIF signal changes <1%. All of the species profiles were obtained with a 10-ns gated integrator and 1,000-shot averaging to minimize the errors due to quenching effects and laser intensity fluctuations. The sampling gate was positioned near the signal peak.

The flame temperatures were measured by NH and OH LIF. The spectra were recorded in a linear energy regime with a 10-ns gate width and fitted using a multiparameter fitting computer program based on a Boltzmann rotational population distribution analysis [9, 10]. Figure 1 shows a typical LIF excitation spectrum of the R branch of the NH $A^3\Sigma^+ - X^3\Pi$ (1,0) transition recorded

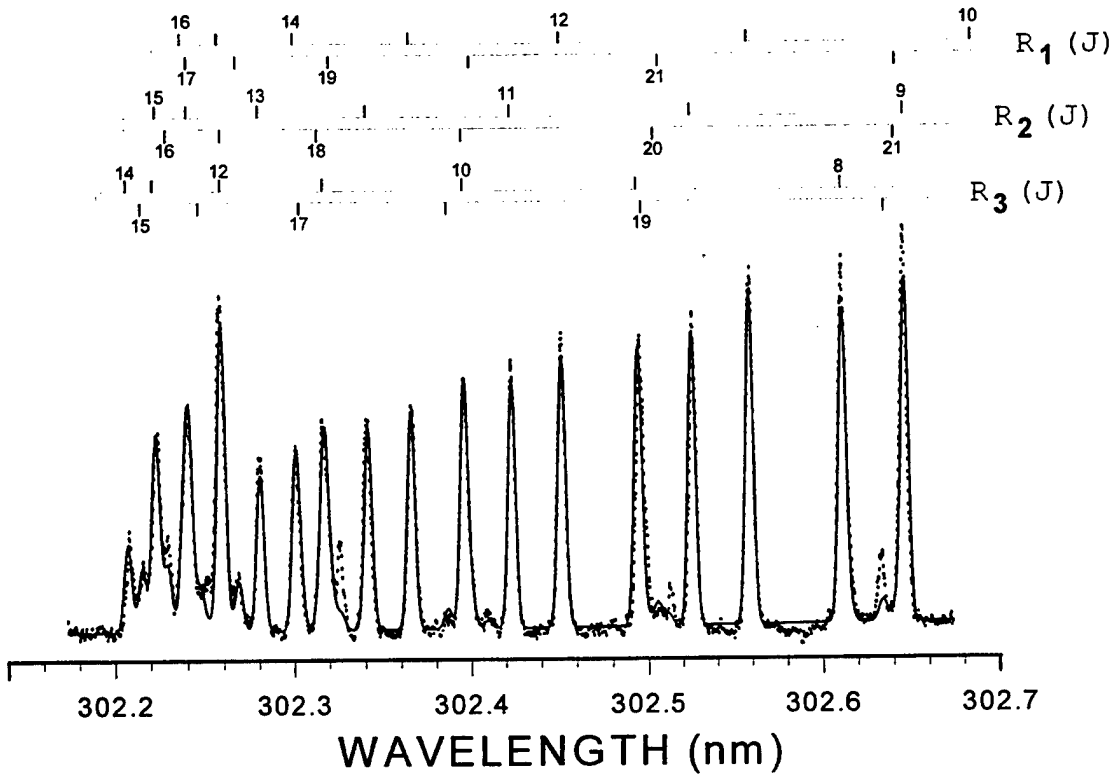

Figure 1. Experimental (...) and Fitted (-) NH Spectra in the 302.2–302.7-nm Region at 5 mm for a 30-Torr H_2/N_2O/Ar Flame Doped With NH_3.

for the NH_3-doped H_2/N_2O/Ar flame. The best fit to the NH LIF spectrum is shown with a solid line and yields a temperature of 1,867 K ±40 K (2SD) at 5 mm.

The flame temperatures were also measured with a thin Pt-Rh (6%)/Pt-Rh (30%) thermocouple that was coated with a beryllium oxide (15%)/yttrium oxide mixture to avoid surface catalytic effects [11]. They were corrected for radiative losses using

$$T_{flame} - T_{meas} = \varepsilon\sigma \frac{d}{h} (T_{meas}^4 - T_\infty^4), \qquad (2)$$

where T_{flame}, T_{meas}, and T_∞ are, respectively, the flame, thermocouple, and ambient temperatures, ε is the thermocouple emissivity, σ the Stefan-Boltzmann constant, and h the convection heat-transfer coefficient between the spherical bead of the thermocouple junction and the flame gases. The

convection coefficient is calculated using the flame temperatures, composition of the flame, and gas velocities for different heights above the burner. Calculations reveal that the correction for the radiative losses is ~350 K in the postflame region, with an experimental uncertainty of ~150 K. As a result of this relatively high uncertainty, the ratio $\varepsilon\sigma/h$ was determined for several different heights above the burner surface using the rotational temperatures obtained from NH LIF measurements in the region near the burner and the OH LIF measurements in the postflame region and then applied to correct the thermocouple temperature profiles in both the neat and NH_3-doped flames. The corrected thermocouple temperature profiles were then fitted with a sigmoid-type function and used in the PREMIX calculations. The corrected thermocouple temperature profiles for the neat and NH_3-doped flames, as well as the temperatures obtained with the LIF technique are shown in Figure 2. The overall uncertainty in the temperature measurements is ±2 and 5% (2SD) for NH and OH LIF, respectively. As shown in Figure 2, when 3.5% of the total flow of NH_3 is added to the a neat $H_2/N_2O/Ar$ flame, the temperature profile is shifted approximately 1 mm away from the burner surface compared to that of the neat flame. Also, the maximum decrease in flame temperature with the NH_3 additive is ~100 K and occurs near the burner surface, while there is no change in the postflame temperatures. NASA-Lewis equilibrium calculations show that when NH_3 is added to the neat flame, the adiabatic flame temperature decreases by 19 K [12].

The species profiles for both neat and NH_3-doped flames were obtained with an in-line triple quadrupole MB/MS (ABB Extrel C50 TQMS) operating at ionization energies from 15–30 eV, depending on the species of interest, to minimize interference from other species. The electron emission current was maintained at 0.1 ±0.01 mA for all the measurements. The profile measurements of the stable species were quantified by introducing calibrated mixtures of the species of interest and Ar in the burner chamber and measuring the ratio of the species to Ar signal intensities at room temperature. With the mass spectrometer settings kept constant, the same ratio of intensities was then measured in the flame. The ratio of the species mole fraction to the Ar mole fraction in the flame was obtained using the following equation:

$$\left(\frac{X_i}{X_{Ar}}\right)_{flame} = \left(\frac{X_i}{X_{Ar}}\right)_{RT} \left(\frac{I_i}{I_{Ar}}\right)_{flame} \left(\frac{I_{Ar}}{I_i}\right)_{RT}, \qquad (3)$$

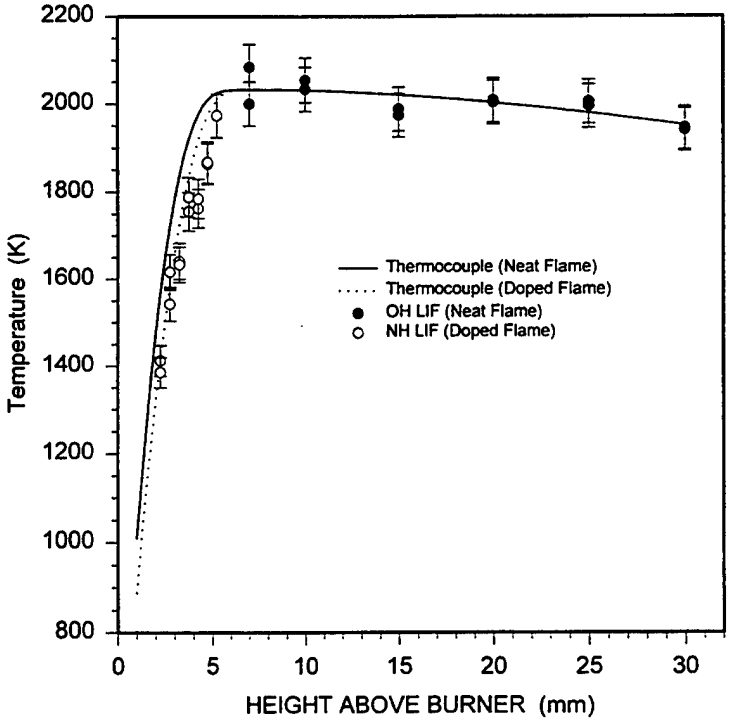

Figure 2. Temperature Profiles for Both Neat and NH_3-Doped Flames. The Flame Temperatures Are Measured by OH LIF for the Neat Flame (●), NH LIF for the Doped Flame (○), and Thin-Wire Thermocouples for Both Neat (-) and Doped (--) Flames. The Thermocouple Measured Temperatures Are Corrected for Radiation Losses Using the LIF Temperatures.

where X_i and I_i are, respectively, the mole fraction and the detected signal intensity for the species of interest. The signal intensity is related to the species mole fraction by $I_i = K_i X_i$, where K_i is an instrument-dependent sensitivity factor. Equation (3) is derived by assuming that (K_i/K_{Ar}) at room temperature (RT) equals (K_i/K_{Ar}) at the flame temperature (flame). The validity of equation (3) was verified in previous work using calibrated mixtures of He and Ar measured under ambient temperature and flame conditions [1, 2, 13]. Equation (3) neglects Mach number focusing that is only significant for H_2. The uncertainty in the MB/MS measurements is 10%.

3. Modeling

The flames were modeled using the Sandia National Laboratories (SNL) flame code PREMIX (ver. 2.55) [14] that employs the CHEMKIN-II (ver. 4.9) chemical kinetics and multicomponent

transport libraries [15, 16], with the measured temperature values and flow rates as input to the flame code, and with several chemical mechanisms involving N-O-H reactions. Two mechanisms served as the basis for all the mechanisms used in the calculations. The first, which is denoted as ***SSLA***, was developed in our laboratory and was published in Sausa et al. [4]. It consists of 87 reactions and 20 species with rate constants obtained from a critical literature review. The second mechanism used is a subset of the benchmark and popular ***GRI 2.11*** mechanism, which was developed for the Gas Research Institute for natural gas ignition and flame. The ***GRI 2.11*** mechanism contains the C-H-O chemistry and it includes the nitrogen chemistry relevant to natural gas chemistry and reburning. All of the carbon-containing species and associated reactions were removed from this mechanism, yielding a subset mechanism consisting of 69 reactions involving 19 species. The two striking differences between the ***SSLA*** and ***GRI 2.11*** mechanisms are that (1) the ***SSLA*** does not contain the NO_2 and H_2O_2 species that are present in the ***GRI 2.11*** mechanism and (2) the ***GRI 2.11*** does not contain the N_2H_2, N_2H_3, and N_2H_4 species that are present in the ***SSLA*** mechanism. All the calculations were performed with both the thermal diffusion and the multicomponent transport package option, and with the normal boundary conditions (i.e., no recombination of H atoms to H_2 via burner surface reaction). Previous work under similar conditions showed that the inclusion of this recombination effect only results in a minor change to the H and H_2 profiles very close to the burner surface. The SNL transport and thermochemical databases were used for the ***SSLA*** calculations, whereas the supplied transport and thermodynamic database default files were used for the ***GRI 2.11*** calculations. A perusal of the thermodynamic databases revealed that the $(\Delta H^\circ_f)_{298}$ values for the same species were within a few tenths of kilocalories/mole of each other, except for NNH. The $(\Delta H^\circ_f)_{298}$ values for this species are 59.6 and 58.5 kcal/mol in the ***GRI 2.11*** and SNL databases, respectively. The effects of the different databases on our calculations were checked by replacing the ***GRI 2.11*** recommended ones with those provided by SNL. The neat flame calculations showed approximately 2 and 1% increase in the respective H_2 and N_2O concentrations at 2.0 mm, and a 0.6 and 0.3 % decrease in the respective H_2O and N_2 concentrations at 15 mm. For the doped flame, the percent change in concentration of the reactants is halved, whereas that of the products is doubled compared to the neat flame. The concentration of OH, NH, and O-atom decreases from 4–12%, with OH showing the least change, for both neat and doped flames. In the neat and doped flame, NO showed approximately a 7 and 11% increase in concentration, respectively, whereas O_2

showed a 15% and 2% decrease in concentration. As expected, the NNH species showed the largest change in concentration, approximately a 41% increase for the neat flame and a 35% increase for the doped flame.

4. Results and Discussion

The modeling results of the neat and NH_3-doped $H_2/N_2O/Ar$ flames using the ***SSLA*** and ***GRI 2.11*** mechanisms reveal that the major species profiles agree well with those observed experimentally, but that the NH_3, O_2, and NH profiles do not. First, the modeling results underpredict the O_2 absolute concentration in the neat flame and do not predict the drop in O_2 concentration with the addition of NH_3. Second, they overpredict NH_3 concentrations throughout the flame for the doped flame. Last, they do not predict the decay of the NH profiles for both neat and NH_3-doped flames. The details in the modeled and experimental profiles is discussed in the latter part of this paper. Insightful information on which reactions to alter in the mechanisms for better prediction of the experimental profiles is obtained by sensitivity analyses.

Presented in Table 1 are the normalized sensitivity coefficients for O_2 at 15.0 mm above the burner surface for both neat and NH_3-doped flames using both the ***SSLA*** and ***GRI 2.11*** mechanisms. The PREMIX code calculates raw sensitivity coefficients for each reaction and species that are then normalized according to the following equation:

$$S_{ik} = (A_i/X_{k,m})\,(\partial X_k/\partial A_i), \tag{4}$$

where S_{ik} is the normalized sensitivity coefficient, A_i is the Arrhenius A coefficient or reaction I, and $X_{k,m}$ is the maximum mole fraction of species k. Positive values indicate that an increase in the reaction rate results in an increase in the species mole fraction, whereas negative values indicate that an increase in the reaction rate results in a decrease in the species mole fraction. As revealed in Table 1, O_2 shows a very strong positive sensitivity to the $N_2O+M=N_2+O+M$ reaction and a negative sensitivity to the $NH+NO=N_2O+H$ reaction for both mechanisms. O_2 also shows a strong sensitivity

Table 1. Sensitivity Coefficients for O_2 in a Neat and NH_3-Doped Flame at 15.0 mm Above the Burner Surface

Reaction	Sensitivity Coefficients (Relative)[a]				
	SSLA			*GRI*	
	Sign	Neat	Doped	Neat	Doped
$N_2O+M=N_2+O+M$	+	100.0	100.0	100.0	100
$NH+NO=N_2O+H$	–	81.6	16.7	81.7	109
$NH+H_2O=HNO+H_2$	–	NP	NP	44.0	310
$NH+OH=HNO+H$	–	49.8	28.0	22.1	74
$NO+N=N_2+O$	+	33.4	26.2	20.7	98
$NO+H=N+OH$	–	30.8	21.8	18.7	75(RR)
$NNH+O=NO+NH$	+	24.3	22.9	18.5	44
$NH+O=NO+H$	–	17.0	7.5	9.2	36
$N_2O+H=OH+N_2$	+	16.3	−101.4	+37.9	+173
$NH+NO=N_2+OH$	+	13.9	<4.5	14.4	59
$H_2+OH=H_2O+H$	–	11.0	59.1	19.9	638
$H+O_2=OH+O$	+	8.4	−26.1	+4.3	−800
$N_2O+O=NO+NO$	–	8.5	<4.5	6.8	2
$H_2+O=H+OH$	–	4.9	30.4	8.7	740
$N_2O+O=N_2+O_2$	+	4.3	17.8	4.6	408
$HNO+H=NO+H_2$	–	3.6	7.5	16.9	29
$NO+H+M=HNO+M$	+	2.7	4.7	8.7	−191
$NH_2+O=HNO+H$	–	2.2	11.5	1.3	154
$OH+OH=H_2O+O$	–	<1	13.8	<1	159
$NH_2+NO=NNH+OH$	+	<1	8.8	NP	NP
$NH_3+OH=NH_2+H_2O$	+	<1	6.8	<1	−64
$NH_2+NH=N_2H_2+H$	+	<1	4.8	NP	NP
$NH+H=N+H_2$	–	<1	<1	+4.7	+239
$NH+OH=N+H_2O$	–	1.5	1.0	+2.3	+77
$HNO+OH=NO+H_2O$	–	1.2	<1	−5.6	<10
$N_2O+OH=N_2+HO_2$	+	<1	<1	1.9	155
$H+HO_2=OH+OH$	–	<1	<1	1.1	90
$NH_3+O=NH_2+OH$	–	<1	1.2	<1	65
$NH+O_2=HNO+O$	–	<1	1.3	<1	18
$H+HO_2=O_2+H_2$	+	<1	<1	<1	36
$OH+HO_2=O_2+H_2O$	+	<1	<1	<1	34

Notes: *SSLA* = neat (100 units = 0.0454), doped (100 units = 0.323).
GRI = neat (100 units = 0.594), doped (100 units = 0.0261).
NP = not present in the mechanism.
RR = reverse reaction.

[a] The sensitivity coefficients is normalized logarithmically using the maximum O_2 mole fraction and then scaled to the $N_2O+M=N_2+O+M$ reaction.

to the NH+OH=HNO+H, NO+N=N_2+O, and NO+H=N+OH reactions for both mechanisms. The reaction NH+H_2O=HNO+H_2, which has an appreciable negative sensitivity coefficient for O_2 in the ***GRI 2.11*** mechanism, is absent from the ***SSLA*** mechanism. When this reaction is included in the ***SSLA*** mechanism, the O_2 and NO concentrations decreased by 56 and 30% in the neat and doped flame, respectively, at 15 mm, increasing the discrepancy between modeled and observed values.

Presented in Figure 3 are the of NH_3 normalized sensitivities as a function of height above burner surface for the doped flame using both the ***SSLA*** and ***GRI 2.11*** mechanisms. NH_3 is very sensitive to N_2O+M=N_2+O+M, N_2O+H=OH+N_2, H_2+OH=H_2O+H, and NH_3+OH=NH_2+H_2O for both ***SSLA*** and ***GRI 2.11*** mechanisms. NH_3 also shows a negative sensitivity to reactions NH_2+NO=NNH+OH and NH_2+NH=N_2H_2+H and a positive sensitivity to OH+NH=HNO+H throughout the flame for the SSLA mechanism. In contrast, NH_3 is not sensitive to the OH+NH=HNO+H reaction for the ***GRI 2.11*** mechanism. The NH_3 sensitivity for reactions NH_2+NH=N_2H_2+H and NH_2+NO=NNH+OH is not displayed for the ***GRI 2.11*** mechanism because they are absent from the mechanism. The NH_2+NO=N_2+H_2O reaction is also not included in the ***GRI 2.11*** mechanism. Another difference between the two mechanisms shown in Figure 3 is that all the NH_3 sensitivity coefficients for the ***SSLA*** mechanism peak at approximately 5 mm and then gradually decrease, reaching ~10% of their values near 25 mm. In contrast, NH_3 shows substantial sensitivity to many reactions above 25 mm for the ***GRI 2.11*** mechanism. Little, if any, NH_3 is observed experimentally above 10 mm.

The O_2 and NH_3 species are very sensitive to the N_2O+M=N_2+O+M reaction as shown in Table 1 and Figure 3, respectively, and an increase in its rate expression will increase the postflame concentration of O_2 and decrease that of NH_3. This trend is in agreement with the experimental results. An increase in the N_2O+M=N_2+O+M reaction's rate expression also decreases the NH concentration for the neat and NH_3-doped flames near the burner surface, as shown in Table 2, and better predicts its decay in both flames. O_2 is also very sensitive to the NH+NO=N_2O+H reaction. A decrease in its rate constant results in an increase in the O_2 postflame concentration, consistent with the experimental results. The NH_3 concentration throughout the flame would not change, however, because NH_3 is insensitive to this reaction. Table 1 also shows that O_2 is sensitive to

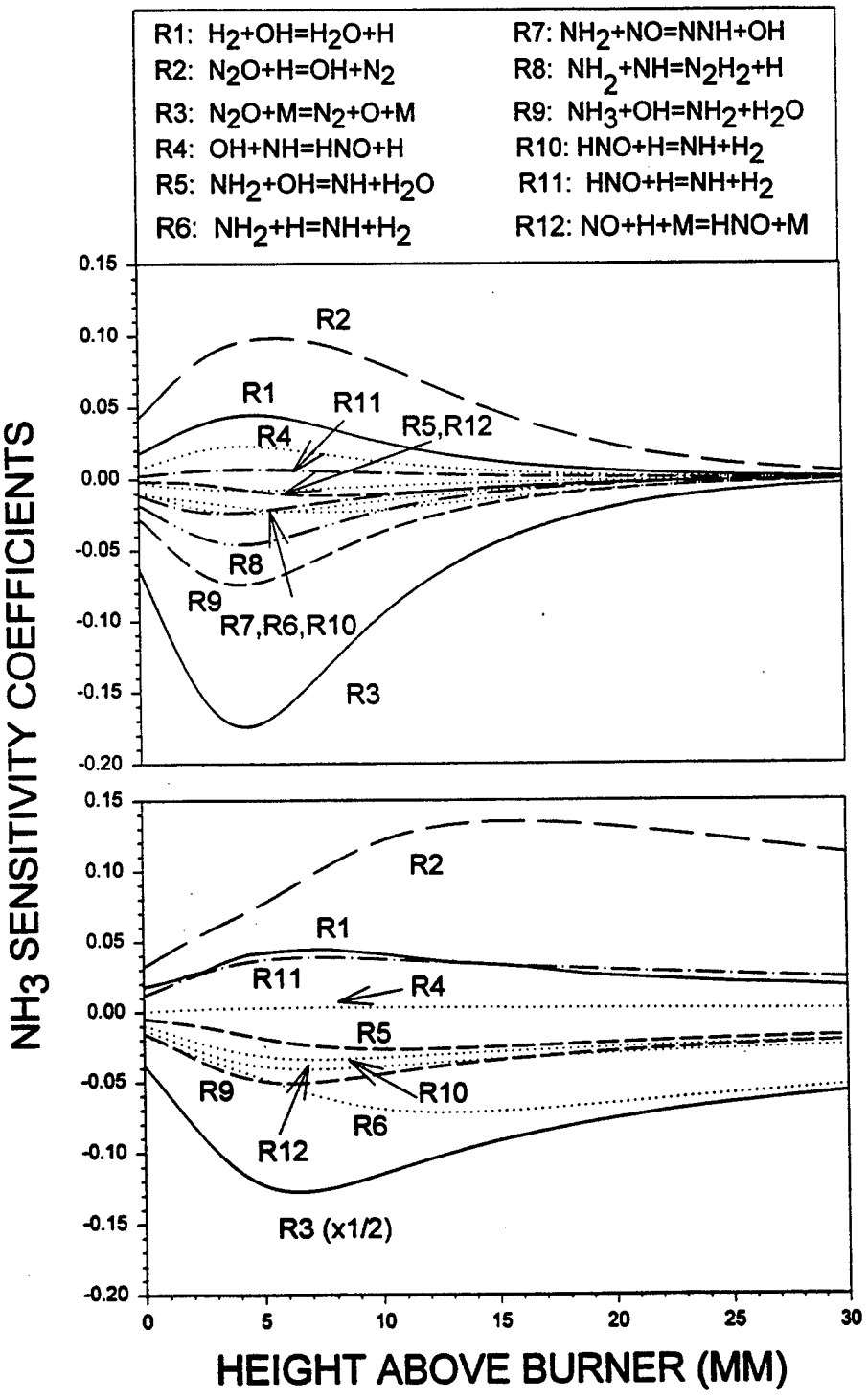

Figure 3. Plot of NH_3 Sensitivity Coefficients as a Function of Height Above Burner for Various Reactions Using Both *SSLA* (Top) and *GRI 2.11* (Bottom) Mechanisms.

Table 2. Sensitivity Coefficients for NH in a Neat and NH_3-Doped Flame at 4.1 and 5.3 mm, Respectively, Above the Burner Surface

Reaction	Sensitivity Coefficients (Relative)[a]				
	SSLA			*GRI*	
	Sign	Neat	Doped	Neat	Doped
$NH+NO=N_2O+H$	+	100.0	99.9	84.5	55.7
$N_2O+H=OH+N_2$	–	92.5	107.1	100.0	100.0
$NH+H_2O=HNO+H_2$	–	NP	NP	28.5	57.0
$N_2O+M=N_2+O+M$	–	37.8	14.8	23.6	8.2
$N+H_2=NH+H$	–	33.3	64.1	22.9	29.4(RR)
$NH+OH=HNO+H$	–	27.6	45.6	16.1	17.9
$H_2+OH=H_2O+H$	+	23.3	22.9	19.3	3.6
$NH+NO=N_2+OH$	–	16.1	18.5	14.9	16.1
$NNH+O=NO+NH$	–	14.2	12.0	8.2	5.4
$NH+OH=N+H_2O$	–	12.7	18.2	11.5	12.0
$NH+NH=N_2+H_2$	–	9.2	42.3	NP	NP
$NH+O=NO+H$	–	8.2	11.3	5.0	8.0
$NO+H=N+OH$	–	4.4	11.4	3.5	8.6(RR)
$NO+N=N_2+O$	+	4.3	18.4	3.1	8.0
$H_2+O=H+OH$	+	2.8	11.9	2.0	10.1
$NH_2+H=NH+H_2$	+	2.7	30.5	2.0	23.8
$NH_2+NH=N_2H_2+H$	–	<1	41.5	NP	NP
$NH_2+OH=NH+H_2O$	+	<1	21.0	<1	12.8
$NH_3+OH=NH_2+H_2O$	+	<1	16.2	<1	19.6
$NH_2+O=HNO+H$	–	<1	10.3	<1	7.4
$NH_2+N=N_2+H+H$	–	<1	7.8	NP	NP
$NH_3+H=NH_2+H_2$	–	<1	<1	<1	9.8
$HNO+H=H_2+NO$	—	—	—	-4.5	-24.7
$H+NO+M=HNO+M$	—	—	—	-5.2	-15.7

Notes: NP = not present in the mechanism.
RR = reverse reaction.

[a] The sensitivity coefficients are normalized logarithmically using the maximum NH mole fraction and then scaled to the NH+NO=N2O+H reaction for the ***SSLA*** mechanism (neat [100 units = 0.518], doped [100 units = 0.0341]) and N2O+H=OH+N2 reaction for the ***GRI*** mechanism (neat [100 units = -0.556], doped [100 units = -0.365]).

reactions $NH+OH=HNO+H$, $NO+N=N_2+O$, and $NO+H=N+OH$, and their rate coefficients could be altered to increase the O_2 postflame concentration. However, these reactions affect the O_2 postflame concentration in NH_3/N_2O flame in a similar manner, and the desired result would be contrary to what is observed experimentally [17]. Thus, the rate expressions for these reactions are

not altered. NH_3 is also sensitive to the $N_2O+H=OH+N_2$ reaction (see Figure 3). A decrease in its rate constant produces a lower NH_3 concentration throughout the flame, in agreement with the experimental results, but also a lower O_2 postflame concentration, contrary to what is observed experimentally. Thus, the rate constant for this reaction is also not altered.

The ***SSLA*** mechanism was modified by altering the rate expression and third body H_2O efficiency for the $N_2O+M=N_2+O+M$ reaction and the rate expression for the $NH+NO=N_2O+H$ reaction. The low-pressure limit rate expression of the $N_2O+M=N_2+O+M$ reaction for N_2 in the ***SSLA*** mechanism is that reported in Röhrig et al. [18], $k = 5.97 \times 10^{14} \exp(-56640/T)$, with a third body H_2O/N_2 efficiency ratio of 7.5 [19]. In contrast, the rate expression in the ***GRI 2.11*** mechanism for N_2 is that reported by Glarborg and coworkers, $k = 6.2 \times 10^{14} \exp(-56100/T)$ with a H_2O/N_2 ratio of 6.0 [20]. This expression is in excellent agreement with that reported by Hanson and Salimian [21]. At the peak temperature in the H_2/N_2O/Ar flame, ~2000 K, the ***GRI 2.11*** value is approximately 26% larger than that used in the ***SSLA*** mechanism. The H_2O and N_2 third-body efficiency values in the ***SSLA*** mechanism are those reported by Glarborg and coworkers [19]. Their values relative to Ar are 12 ±3.5 and 1.7 ±0.3, respectively, in the 1,000–1,400-K range. The ***SSLA*** mechanism is thus modified to include the rate constant expression from the ***GRI 2.11*** mechanism, with an effective H_2O/N_2 ratio of 11, the upper value of experimental uncertainty reported by Glarborg and coworkers [19]. A similar effect in the modeling results can be achieved by using the rate constant reported in Röhrig et al. [18] with a larger effective ratio for H_2O/N_2, which is certainly plausible for our flame conditions.

The rate expression for the $NH+NO=N_2O+H$ reaction in the ***SSLA*** mechanism is that obtained by Miller and Melius [22] from BAC-MP4 calculations, $k = 2.94 \times 10^{14} T^{-0.40} - 2.16 \times 10^{13} T^{-0.23}$. In the ***SSLA modified*** mechanism, it is decreased by 25%, certainly within the theoretical uncertainty. For comparison purposes, the rate expression in the ***GRI 2.11*** mechanism, $k = 4.16 \times 10^{14} T^{-0.45}$, yields a rate constant at 2,000 K, which is approximately 32% greater than that used in the ***SSLA***. This reaction strongly affects both the ***SSLA*** and ***GRI 2.11*** calculated postflame NO concentration. Calculations for the neat flame using both mechanisms show that the NO sensitivity coefficient for this reaction is positive and is second (55%) to that of the $N_2O+H=OH+N_2$ (100%) reaction in

absolute value. In the doped flame, the ***SSLA*** and ***GRI 2.11*** sensitivity coefficients for the $NH+NO=N_2O+H$ reaction are ~33% less than that of the $N_2O+H=OH+N_2$ reaction.

Four different sets of calculations are performed for neat and NH_3-doped flames: (1) ***SSLA*** - uses the SSLA mechanism and the measured temperature profile as input; (2) ***GRI 2.11*** - uses the ***GRI 2.11*** mechanism and the measured temperature profile as input; (3) ***SSLA modified*** - uses the SSLA mechanism in which the $N_2O+M=N_2+O+M$ and $NH+NO=N_2O+H$ reactions are altered, as discussed previously, and a 5% increase in the temperature profile as input (twice the standard deviation of our experimental uncertainty); and (4) ***GRI 2.11 modified*** - uses the ***GRI 2.11*** mechanism in which the aforementioned two reactions are altered as in the ***SSLA*** mechanism and a 5% increase in the temperature profile as input. The modified ***GRI 2.11*** mechanism is not optimized, and the calculations are included for comparison purposes.

The H_2, N_2O, H_2O, and N_2 calculated profiles for both the neat and NH_3-doped H_2/N_2O/Ar flames agree well with those obtained experimentally using all four mechanisms. The calculated NH_3 profiles for the doped flame, along with the experimental profile, are shown in Figure 4. The experiment and model calculations show a negligible mole fraction for the NH_3 in the neat flame. The ***SSLA modified*** model overpredicts the NH_3 by 6% near the burner surface, which is within the experimental uncertainty of the measurement. The model also indicates that, at the height of 15 mm (postflame region), the NH_3 dopant decreases to a level of 0.6% of the added amount, similar to that observed experimentally. In contrast, the ***SSLA*** calculations reveal that the calculated NH_3 mole fraction (at 15 mm) decreases to 3% of the added amount. Calculations using the ***modified GRI*** mechanism also predict this result. The NH_3 profile calculated with the ***GRI*** mechanism has the maximum deviation from the experimental results, as shown in Figure 3, and shows 15% of NH_3 remaining unconsumed in the postflame region.

Rate analysis for the ***SSLA modified*** calculations reveal that all of the NH_3 is consumed by the $NH_3+OH=NH_2+H_2O$, $NH_3+H=NH_2+H_2$, and $NH_3+O=NH_2+OH$ reactions, the first accounting for ~86% of its consumption. The reactions $NH_3+M=NH_2+H+M$, $NH_2+NH_2=NH+NH_3$, and

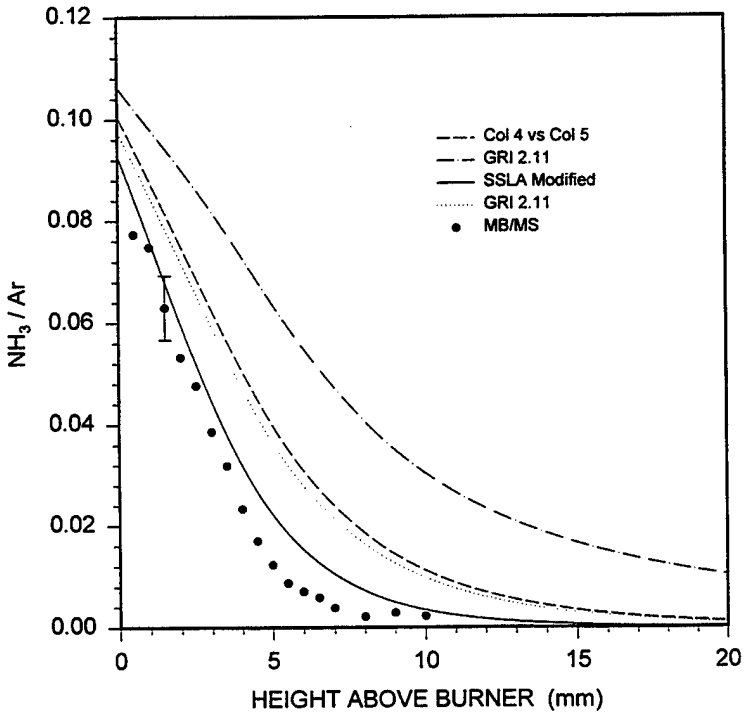

Figure 4. Experimental and Modeled NH_3 Profiles.

$HNO+NH_3=NH_3+NO$ account for most of its formation, but their total rate is ~3.8% of the consumption rate.

The experimental and modeled O_2 profiles for the neat and NH_3-doped flames are shown in Figure 5. The MB/MS measurements reveal a 90% decrease in O_2 in the burnt gas region of the NH_3-doped flame. The ***SSLA modified*** modeling results show that the amount of O_2 formed in the doped flame decreases by 86% and underpredicts the O_2 formation in the neat flame by 5% at 15 mm. The ***modified GRI 2.11*** mechanism also underpredicts the amount of O_2 in the neat flame by 13%, but shows a relative drop in the doped flame of 90%. Overall, both of the aforementioned mechanisms well predict the shape of the O_2 profiles. However, the ***modified GRI 2.11*** results display a more pronounced decay in O_2 profile in the burnt gas region of the doped flame. The ***SSLA*** and ***GRI 2.11*** display the maximum deviation (39% and 57%, respectively) from the measured O_2 mole fraction in the neat flame.

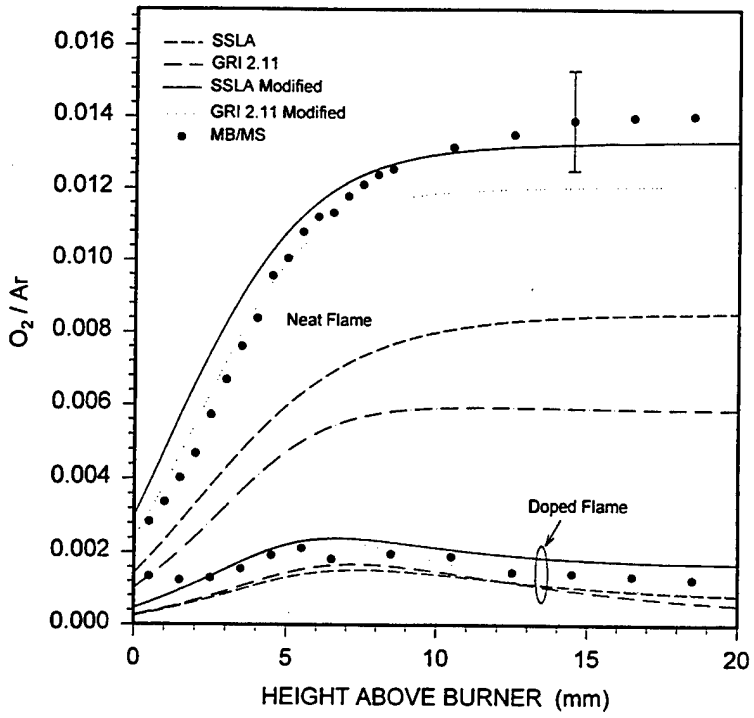

Figure 5. Experimental and Modeled O_2 Profiles.

Presented in Figure 6 are the major reactions forming and consuming O_2, along with the total O_2 rate, for both neat and NH_3-doped flames. For the neat flame, all of the O_2 is produced by the $N_2O+O=N_2+O_2$ and $H+O_2=OH+O$ reactions. Reactions $NO+O=N+O_2$ and $NH+O_2=HNO+O$ contribute slightly toward its consumption, whereas the $O_2+H+M=HO_2+M$ reaction has little effect on both its formation or consumption. For the doped flame, the $N_2O+O=N_2+O_2$ reaction also forms O_2 and the $H+O_2=OH+O$ reaction forms O_2 up to 7.5 mm and consumes it at distances greater than 7.5 mm. Reactions $NO+O=N+O_2$ and $NH+O_2=HNO+O$ contribute slightly toward O_2 consumption, as in the neat flame, but are approximately 50% less effective. The net integrated rate of O_2 production (0–20 mm) in the neat flame is thus ~10 times larger than that in the doped flame primarily because the $N_2O+O=N_2+O_2$ reaction has a smaller positive contribution in the doped flame and because the $H+O_2=OH+O$ reaction has a smaller positive contribution at distances <7.5 mm and a negative contribution at distances >7.5 mm.

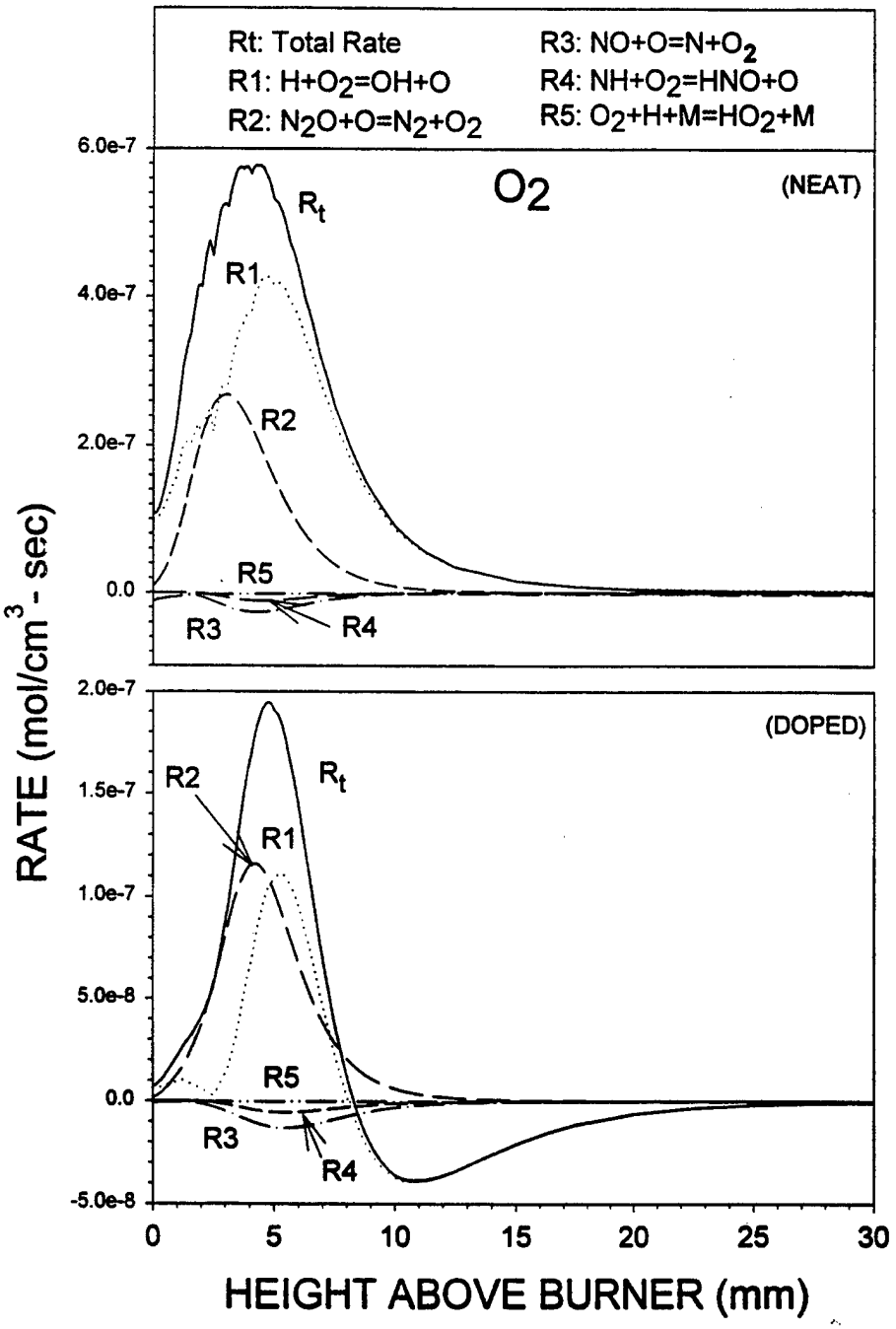

Figure 6. O_2 Reaction Rates From *SSLA Modified* Calculations for Both Neat and NH_3-Doped H_2/N_2O/Ar Flames.

It should be noted that the rate expression for the $N_2O+O=N_2+O_2$ reaction used in the ***SSLA modified*** mechanism is that reported by Hanson and coworkers [23], $k = 1.40 \times 10^{12} \exp(-10{,}800/T)$. Altering this rate expression to that recommended by Hanson and Salimian [21], $k = 1.0 \times 10^{14} \exp(-28{,}020/T)$ results in a negligible change in the computed O_2 and NO mole fractions for both neat and NH_3-doped flames at 15 mm. In addition, the net integrated rate of O_2 production for both neat and doped flames is hardly changed. The peak rate for this reaction is, however, decreased by approximately 32 and 25% for neat and doped flames, respectively, and it shifted approximately 1 mm away from the burner surface for both flames.

Figure 7 shows the NO/Ar ratio measured by MB/MS in the neat and doped flame. For comparison purposes, the NO profiles obtained with LIF are converted to NO/Ar ratio using the measured temperatures and the calculated Ar mole fractions. The NO/Ar (LIF) profile is then normalized to the calibrated MB/MS value in the neat flame. The LIF from NO is also quantified by calibrating the NO fluorescence signals using LIF measurements from calibrated mixtures of NO and Ar at room temperature. The analysis incorporates the change in the Boltzmann fraction of the ground level due to the temperature difference between the calibration and the flame conditions. The LIF value is approximately 50% lower than the MB/MS value, within the experimental uncertainty of the LIF measurement. A similar NO LIF uncertainty is reported by Heard et al. [24] for a 30-Torr CH4/Air flame. The MB/MS measurements show a decrease of 32% in the NO when NH_3 is added, whereas the LIF measurements show a decrease of 35%. Considering the experimental uncertainties involved, both the LIF and MB/MS measurements show the same level of NO depletion in the doped flame. The ***SSLA modified*** calculations predict a 38% drop in the level of NO between the neat and NH_3-doped flames, in excellent agreement with that observed experimentally. The calculations also underpredict slightly the NO mole fraction in both the neat and doped flame. All of the calculations used in this study well predict the shape of the NO profiles and the mole fraction of NO in the neat flame. The relative decrease in NO with NH_3 doping is well predicted, however, only by the ***SSLA modified*** and ***GRI 2.11*** models.

Figure 8 shows key reactions contributing to NO production and consumption, along with the total rate, for both neat and NH_3-doped flames. As expected, the peak rate of production at

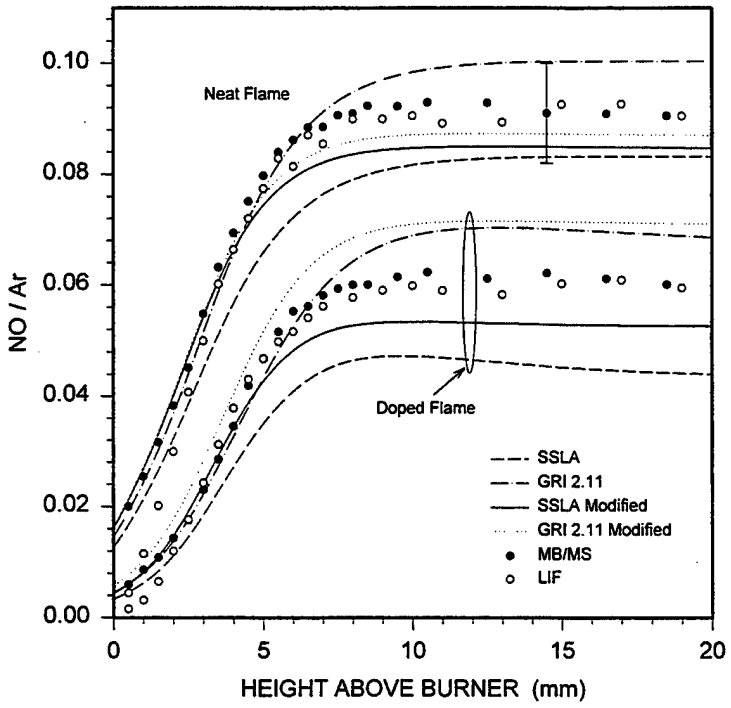

Figure 7. Experimental and Modeled NO Profiles for Neat and NH_3-Doped H_2/N_2O/Ar Flames. The Experimental Profiles Are Obtained by MB/MS (●) and LIF (○).

approximately 5 mm corresponds to the maximum temperature rise. The net integrated rate (0–30 mm) of NO production for the neat flame is approximately 2.4×10^{-06} mol/cm^2-s. Reactions NH+NO=N_2O+H, HNO+H=NO+H_2, and NO+H=N+OH account for 86% of the NO production flux, whereas reactions NO+N=N_2+O, NH+NO=N_2+OH, and NNH+O=NO+NH account for over 99% of the NO consumption flux. The addition of NH_3 to the neat flame results in a net integrated rate of 1.46×10^{-06} mol/cm^2-s, a decrease of ~42% from the neat flame. This decrease is primarily from the NH+NO=N_2O+H reaction. The HNO+H=NO+H_2 and NO+H=N+OH reactions produce more NO in the doped flame compared to the neat flame. Consumption of NO from reactions NO+N=N_2+O, NH+NO=N_2+OH, and NNH+O=NO+NH is also greater in the doped flame compared to the neat flame. In addition, the integrated reaction rates for the NH_2+NO=NNH+OH and NH_2+NO=N_2+H_2O reactions are approximately 20 times greater in the doped flame compared to the neat flame, accounting for ~16% of the consumption of NO in the doped flame.

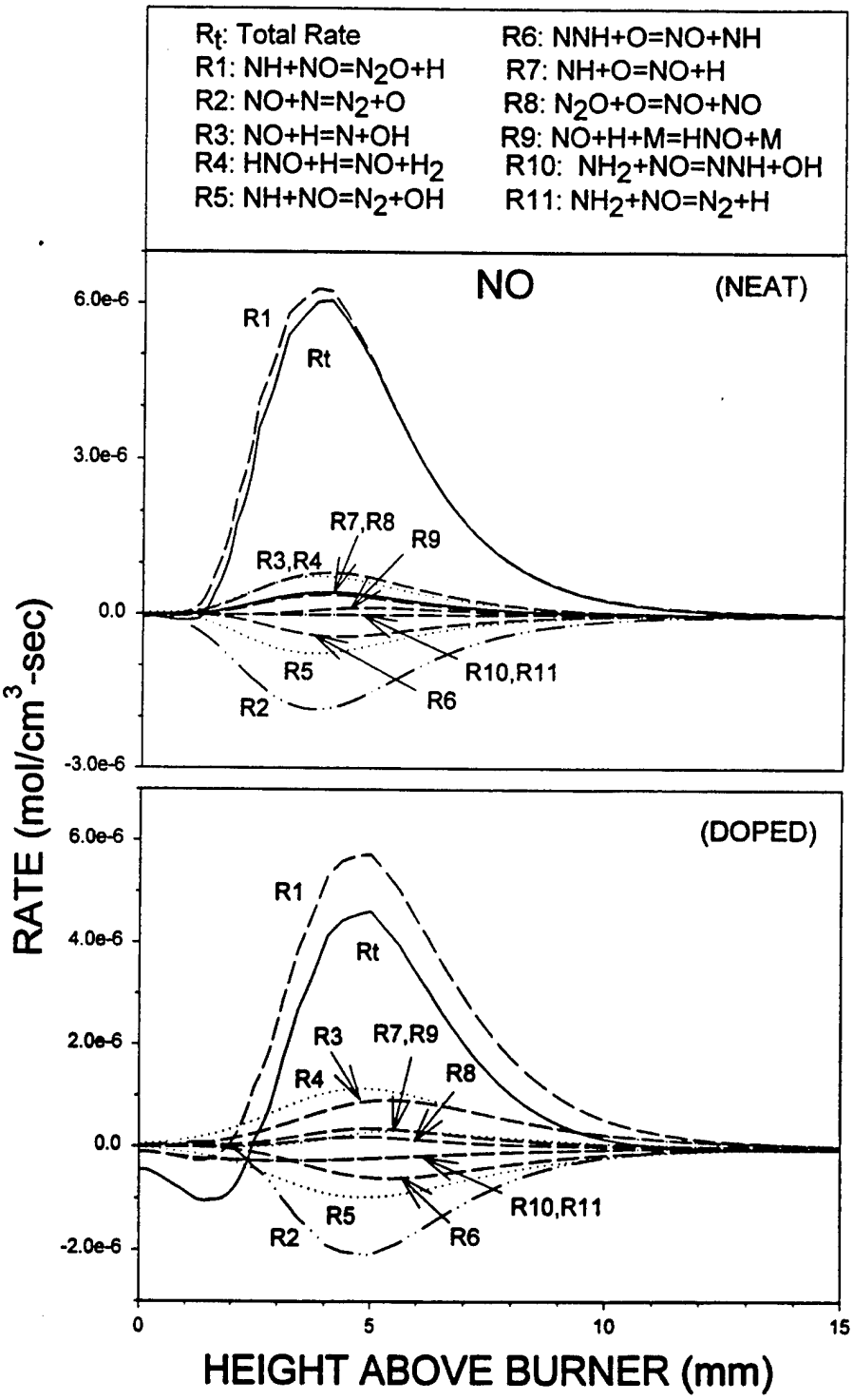

Figure 8. Reaction Rates of NO From *SSLA Modified* Calculations for Both Neat and NH_3-Doped H_2/N_2O/Ar Flames.

Figure 9 shows the calculated and the experimental NH profiles. The experimental and calculated relative NH profiles are normalized to unity for the neat flame. The ***modified SSLA*** model predicts a 126% increase in NH when NH_3 is added to the flame. This agrees well with the 109% increase measured by LIF. The ***SSLA*** model calculations predict an 89% increase in NH with NH_3 doping, whereas the ***GRI 2.11*** and ***modified GRI 2.11*** calculations predict a 95% and 159% increase, respectively. The predicted NH peaks are at 3.75 mm for the neat and 4.75 mm for the doped flames, in agreement with the experimental peaks at 3.5 and 4 mm for the neat and doped flame, respectively. The ***SSLA modified*** calculations well predict the shape of NH profile in the neat flame, including the position of its peak concentration. The calculations also well predict the relative increase in NH concentration as the neat flame is doped with NH_3. For the doped flame, all the calculations show a broader NH peak than that observed experimentally, with the ***SSLA modified*** results agreeing best.

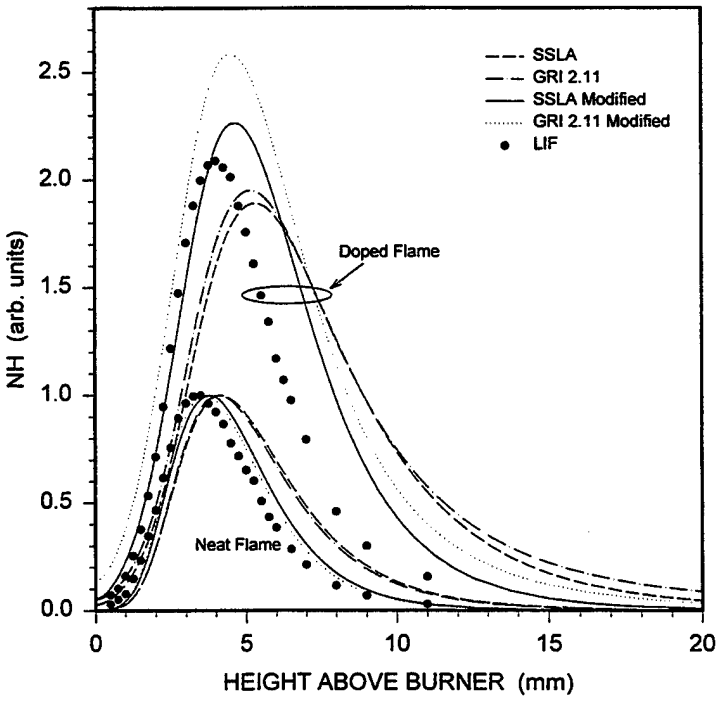

Figure 9. NH Experimental and Modeled Profiles for Neat and NH_3-Doped $H_2/N_2O/Ar$ Flames. The Experimental Concentration Profiles Are Converted to Mole Fraction Using the Experimental Temperature Profile. All the Profiles for the Neat Flame Are Normalized to Unity. Their Peak Mole Fraction Values Are 2.257×10^{-4}, 1.972×10^{-4}, 1.816×10^{-4}, and 1.393×10^{-4} for the *SSLA*, *GRI 2.11*, *SSLA Modified*, and *GRI 2.11 Modified* Calculations, Respectively.

The ***SSLA modified*** calculations rate analyses results are presented in Figure 10. The integrated rates (0–30 mm) for the neat flame show that almost all of the NH is formed from the $NH+NO=N_2O+H$ reaction and 64% is consumed from the $N+H_2=NH+H$, $NH+OH=HNO+H$, and $NH+NO=N_2+OH$ reactions. For the doped flame, the $NH+NO=N_2O+H$ reaction still plays a key role in NH formation. However, the $NH_2+H=NH+H_2$ and $NH_2+OH=NH+H_2O$ reactions are also important and account for ~48% of the NH production. In contrast, these reactions form <1% NH in the neat flame. The reactions $N+H_2=NH+H$, $NH+OH=HNO+H$, $NH+NO=N_2+OH$ and $NH+OH=N+H_2O$ are important for NH consumption in the doped flame, as in the neat flame, with the integrated (0–30 mm) $N+H_2=NH+H$ reaction rate being a factor of 2 larger than that of the neat flame.

The experimental and modeled OH profiles for the neat and NH_3-doped flame are shown in Figure 11. All the calculated OH profiles for the neat flame were also normalized to unity. The shape of the OH profiles are predicted very well by the ***SSLA modified*** model. The calculations show a 53% drop in the OH in the burnt gas region of the flame when NH_3 is added, which agrees rather well with the experimental decrease of 43%. As shown in Figure 11, using the other three mechanisms results in the OH profile decaying in postflame region, with the ***GRI 2.11*** results being the most pronounced. These mechanisms also overpredict the percent decrease in the amount of OH with NH_3 doping. Rate analyses of the ***SSLA modified*** calculations reveal that in the neat flame OH is formed primarily from the $N_2O+H=OH+N_2$ reaction and consumed by the $H_2+OH=H_2O+H$ reaction, as expected. The $H_2+O=H+OH$ reaction also plays a lesser, but an important role in the OH formation. For the doped flame, the aforementioned reactions also play key roles in the production and consumption of OH. The $NH_3+OH=NH_2+H_2O$ also accounts for ~9% of the OH consumption in the doped flame, compared to the neat flame in which it plays a minor role.

The experimental and calculated relative concentration profiles for the O-atom are shown in Figure 12. Overall, the models fairly well predict the shape of the O-atom profile in the neat flame. However, none of the models predict the 10% decay observed in the O-atom concentration profile in the postflame region. In fact, all of the calculated profiles exhibit a plateau in this region. The ***modified SSLA*** calculations show the best agreement in the decrease in the O-atom concentration

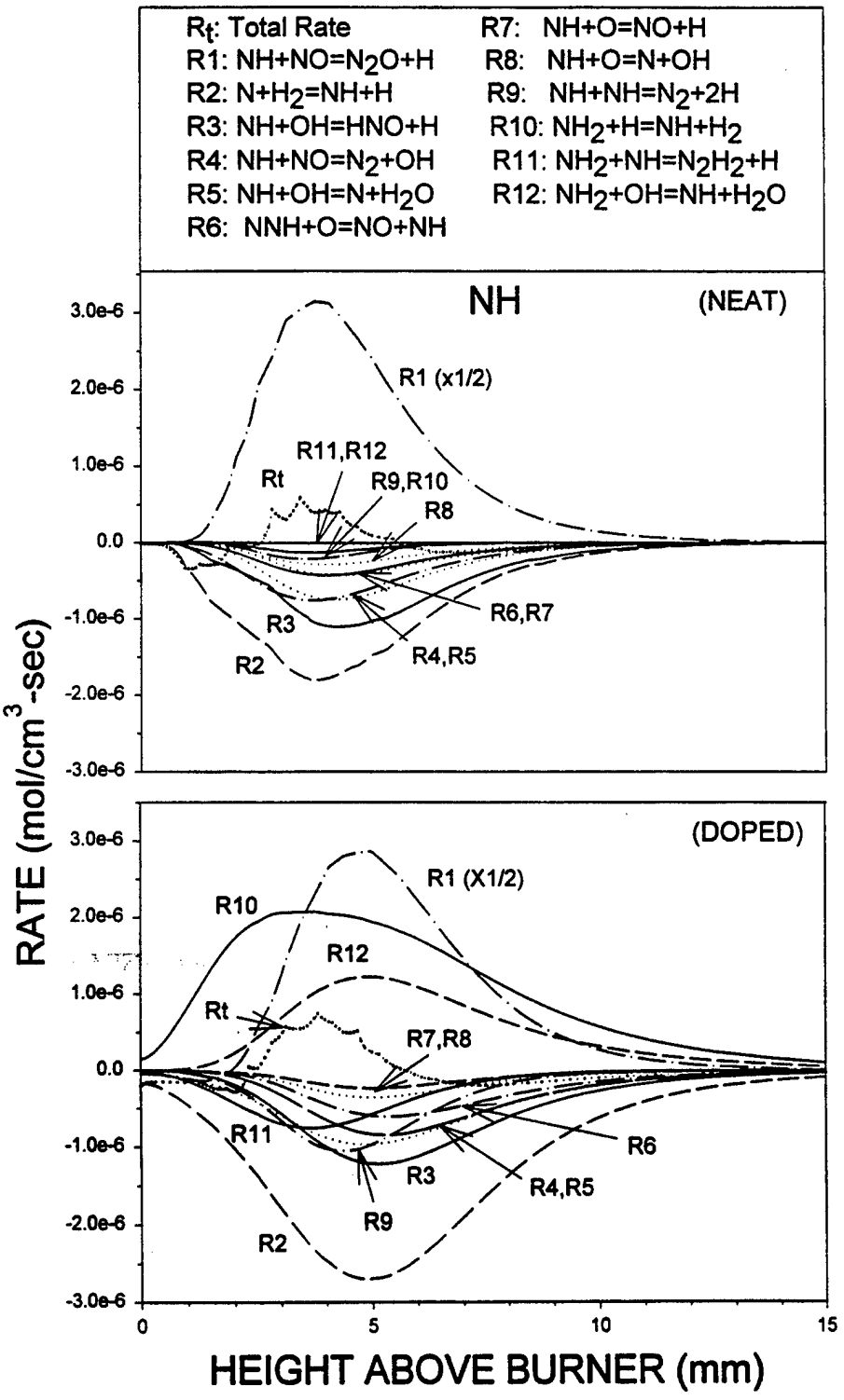

Figure 10. NH Reaction Rates From *SSLA Modified* Calculations for Both Neat and NH_3-Doped H_2/N_2O/Ar Flames.

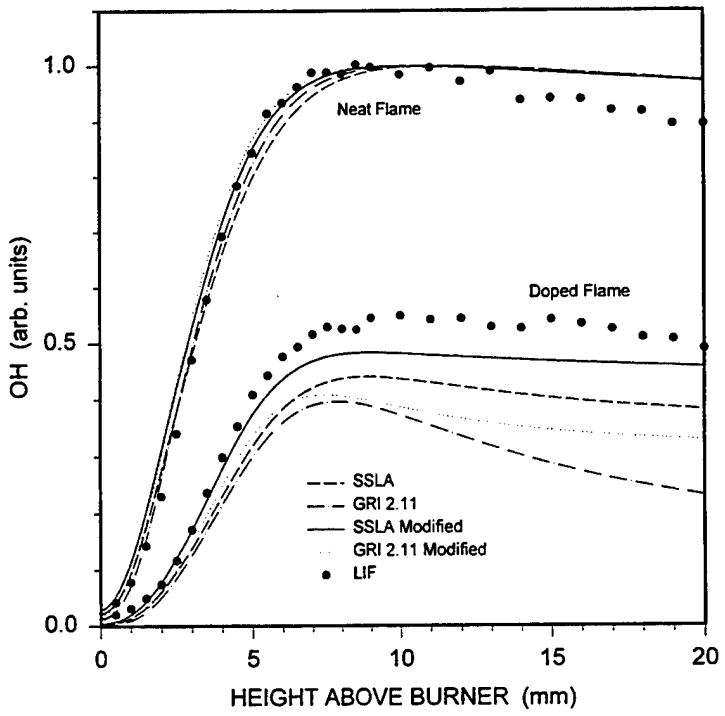

Figure 11. OH Experimental and Modeled Profiles for Neat and NH_3-Doped $H_2/N_2O/Ar$ Flames. The Experimental Concentration Profiles Are Converted to Mole Fraction Using the Experimental Temperature Profile. All the Profiles for the Neat Flame Are Normalized to Unity. Their Mole Fraction Values at 15 mm Are 9.932×10^{-3}, 4.140×10^{-3}, 7.211×10^{-3}, and 6.689×10^{-3} for the *SSLA*, *GRI 2.11*, *SSLA Modified*, and *GRI 2.11 Modified* Calculations, Respectively.

in the postflame region when NH_3 is added. A 77% decrease is calculated compared to a 68% decrease measured by LIF. The models do not very well predict the shape of the O-atom profile in the doped flame. All of the mechanisms used in the modeling of the flames show a slower chemistry than experimentally observed (i.e., the calculated profiles are shifted away from the burner) especially in the doped flame. One possible explanation of this effect is photochemical interference from O-atom [25]. Our experimental findings do not support this explanation, however, because there should be a decrease and not an increase in the interference effects in the doped flame, where the amount of O_2 present is greatly reduced. Alternative explanations include photochemical effects for other O-atom-containing species and/or further refinements of the modified SSLA mechanism. Experiments and PREMIX calculations along these lines are ongoing.

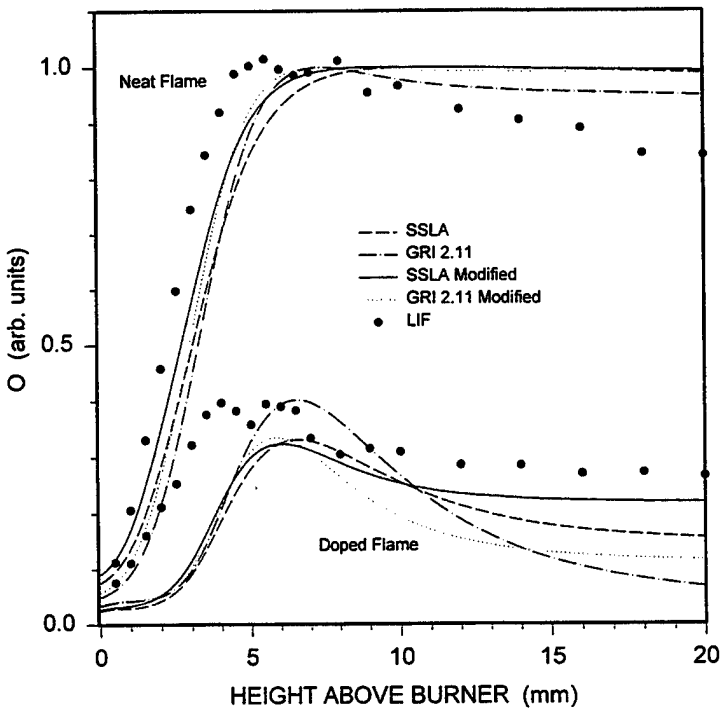

Figure 12. O-Atom Experimental and Modeled Profiles for Neat and NH_3-Doped H_2/N_2O/Ar Flames. The Experimental Concentration Profiles Are Converted to Mole Fraction Using the Experimental Temperature Profile. All the Profiles for the Neat Flame Are Normalized to Unity. Their Mole Fraction Values at 15 mm Are 5.125×10^{-4}, 3.826×10^{-4}, 9.180×10^{-4}, and 8.2411×10^{-4} for the *SSLA*, *GRI 2.11*, *SSLA Modified*, and *GRI 2.11 Modified* Calculations, Respectively.

5. Conclusion

A combined experimental and modeling study of neat and NH_3-doped H_2/N_2O flames has been performed. Species concentrations were measured by MB/MS and/or LIF, and flame temperatures were measured by both OH and NH LIF and thin-wire thermometry. The experimental profiles were compared with calculated profiles generated using PREMIX with the following detailed chemical mechanisms: (1) ***SSLA***, (2) ***modified SSLA***, (3) ***GRI 2.11***, and (4) ***modified GRI 2.11***. Overall, the major experimental species profiles for both neat and NH_3-doped flames are predicted fairly well using all four mechanisms. The minor species profiles are modeled best, however, using the ***modified SSLA*** mechanism. In this mechanism the rate expression for the $NH+NO=N_2O+H$

reaction is decreased by 25%, the rate expression for the $N_2O+M=N_2+O+M$ reaction is increased 25%, and the H_2O third-body efficiency for the latter reaction increased ~47%, the upper limit of the experimental uncertainty. The ***modified SSLA*** calculations rather well predict the species profiles for both neat and doped flames, as well as the increase in postflame O_2, NO, OH, and O-atom concentrations, and the increase in the peak NH concentration with the addition of 4% NH_3. The calculations show a decrease of 38% in NO, 36% in O_2, 53% in OH, and 77% in the O-atom, and an increase of 126% in NH, compared to a decrease of 32 and 35% in NO measured by LIF and MB/MS, respectively, and a decrease of 90% in O_2, 43% in OH, and 68% in the O-atom and an increase of 109% in NH measured by LIF. The NH and O-atom profiles for the neat flame are also predicted the best and fairly well by the ***modified SSLA***. For the doped flame, however, all mechanisms predict a broader NH profile and an O-atom profile that is shifted ~2 mm away from the burner compared to that measured experimentally. These discrepancies are presently under investigation.

6. References

1. Sausa, R. C., W. R. Anderson, D. C. Dayton, C. M. Faust, and S. L. Howard. *Combustion and Flame*. Vol. 94, p. 407 (references therein), 1993.

2. Dayton, D. C., C. M. Faust, W. R. Anderson, and R. C. Sausa. *Combustion and Flame*. Vol. 99, p. 323 (references therein), 1994.

3. Vandooren, J., P. J. Van Tiggelen, and J.-F. Pauwels. *Combustion Science and Technology*. Vol. 109, p. 647, 1997.

4. Sausa, R. C., G. Singh, G. W. Lemire, and W. R. Anderson. *Proceedings of the Twenty-Sixth (International) Symposium on Combustion*. The Combustion Institute, p. 1043, 1996.

5. Bowman, C. T., R. K. Hanson, D. F. Davidson, W. C. Gardiner, V. Lissianski, C. P. Smith, D. M. Golden, M. Frenklach, and M. Goldenberg. Internet address: http://www.me.berkeley.edu/gri_mech.

6. Cattolica, R. J., S. Yoon, and E. L. Knuth. Paper 88. Western States Section/Combustion Institute, 1980.

7. Zabarnick, S. *Combustion Science and Technology*. Vol. 83, p. 115, 1992.

8. Eckbreth, A. C. *Laser Diagnostics for Combustion Temperature and Species*. Abacus Press, MA, 1988.

9. Vanderhoff, J. A., M. W. Teague, and A. J. Kotlar. *Proceedings of the Twenty-Fourth Symposium (International) on Combustion*. The Combustion Institute, p. 1915, 1992.

10. Vanderhoff, J. A., and A. J. Kotlar. BRL-MR-3866, U.S. Army Ballistic Research Laboratory, Aberdeen Proving Ground, MD, 1990.

11. Kent, J. H. *Combustion and Flame*. Vol. 14, p. 279, 1970.

12. Svehla, R. A., and B. J. McBride. NASA-TN-D-7057. January 1973.

13. Howard, S. L., J. E. Newberry, R. C. Sausa, and A. W. Miziolek. *Journal of American Society Mass Spectrometry*. Vol. 4, p. 152, 1993.

14. Kee, R. J., J. F. Crcar, M. D. Smooke, and J. A. Miller. SAND85-8240, Sandia National Laboratory, 1985.

15. Kee, R. J., J. Warnatz, and J. A. Miller. SAN83-8209, Sandia National Laboratory, 1993.

16. Kee, R. J., F. M. Rupley, and J. A. Miller. SAND87-8215, Sandia National Laboratory, 1987.

17. Venizelos, D., and R. Sausa. To be published.

18. Röhrig, M., E. L. Petersen, D. F. Davidson, and R. K. Hanson. *International Journal of Chemical Kinetics*. Vol. 28, p. 599, 1996.

19. Glarborg P., J. E. Johnsson, and K. Dam-Johansen. *Combustion and Flame*. Vol. 99, p. 523, 1994.

20. Johnsson, J. E., P. Glarborg, and K. Dam-Johansen. *Proceedings of the 24th International Symposium on Combustion*. The Combustion Institute, p. 917, 1992.

21. Hanson, R. K., and S. Salimian. "Survey of Rate Constants in the N/H/O System." *Combustion Chemistry*, ch. 6, N. C. Gardiner (editor), Springer Verlorg, NY, 1985.

22. Miller, J. A., and C. F. Melius. *Proceedings of the Twenty-Fourth Symposium (International) on Combustion*. The Combustion Institute, p. 719, Pittsburgh, 1992.

23. Davidson, D. F., M. D. DiRosa, A. Y. Chang, and R. K. Hanson. "Shock Tube Measurements of the Major Product Channels of N_2O + O." *Shock Waves*, vol. 2, p. 813, K. Takayama (editor), Springer Verlag, NY, 1992.

24. Heard, D. E., J. B. Jeffries, G. P. Smith, and D. R. Crosley. *Combustion and Flame*. Vol. 88, p. 137, 1992.

25. Westblom, U., F. Fernadez-Alonso, C. R. Mahon, G. P. Smith, J. B. Jeffries, and Crosley. *Combustion and Flame*. Vol. 99, p. 261, 1994.

NO. OF COPIES ORGANIZATION

2 DEFENSE TECHNICAL INFORMATION CENTER
DTIC DDA
8725 JOHN J KINGMAN RD
STE 0944
FT BELVOIR VA 22060-6218

1 HQDA
DAMO FDQ
D SCHMIDT
400 ARMY PENTAGON
WASHINGTON DC 20310-0460

1 OSD
OUSD(A&T)/ODDDR&E(R)
R J TREW
THE PENTAGON
WASHINGTON DC 20301-7100

1 DPTY CG FOR RDE HQ
US ARMY MATERIEL CMD
AMCRD
MG CALDWELL
5001 EISENHOWER AVE
ALEXANDRIA VA 22333-0001

1 INST FOR ADVNCD TCHNLGY
THE UNIV OF TEXAS AT AUSTIN
PO BOX 202797
AUSTIN TX 78720-2797

1 DARPA
B KASPAR
3701 N FAIRFAX DR
ARLINGTON VA 22203-1714

1 NAVAL SURFACE WARFARE CTR
CODE B07 J PENNELLA
17320 DAHLGREN RD
BLDG 1470 RM 1101
DAHLGREN VA 22448-5100

1 US MILITARY ACADEMY
MATH SCI CTR OF EXCELLENCE
DEPT OF MATHEMATICAL SCI
MAJ M D PHILLIPS
THAYER HALL
WEST POINT NY 10996-1786

NO. OF COPIES ORGANIZATION

1 DIRECTOR
US ARMY RESEARCH LAB
AMSRL D
R W WHALIN
2800 POWDER MILL RD
ADELPHI MD 20783-1145

1 DIRECTOR
US ARMY RESEARCH LAB
AMSRL DD
J J ROCCHIO
2800 POWDER MILL RD
ADELPHI MD 20783-1145

1 DIRECTOR
US ARMY RESEARCH LAB
AMSRL CS AS (RECORDS MGMT)
2800 POWDER MILL RD
ADELPHI MD 20783-1145

3 DIRECTOR
US ARMY RESEARCH LAB
AMSRL CI LL
2800 POWDER MILL RD
ADELPHI MD 20783-1145

ABERDEEN PROVING GROUND

4 DIR USARL
AMSRL CI LP (305)

NO. OF
COPIES ORGANIZATION

ABERDEEN PROVING GROUND

42 DIR, USARL
AMSRL-WM-B,
A.W. HORST
AMSRL-WM-BD,
B.E. FORCH
G.F. ADAMS
W.R. ANDERSON
R.A. BEYER
S.W. BUNTE
C.F. CHABALOWSKI
S. COLEMAN
A. COHEN
R. CUMPTON
R. DANIEL
D. DEVYNCK
R.A. FIFER
J.M. HEIMERL
B.E. HOMAN
A. JUHASZ
A.J. KOTLAR
R. KRANZE
E. LANCASTER
W.F. MCBRATNEY
K.L. MCNESBY
M. MCQUAID
N.E. MEAGHER
M.S. MILLER
A.W. MIZIOLEK
J.B. MORRIS
J.E. NEWBERRY
S.V. PAI
R.A. PESCE-RODRIGUEZ
J. RASIMAS
P. REEVES
B.M. RICE
P. SAEGAR
R.C. SAUSA (2 CP)
M.A. SCHROEDER
R. SCHWEITZER
L.D. SEGER
J.A. VANDERHOFF
D. VENIZELOS
A. WHREN
H.L. WILLIAMS

REPORT DOCUMENTATION PAGE

Form Approved
OMB No. 0704-0188

1. AGENCY USE ONLY *(Leave blank)*	2. REPORT DATE	3. REPORT TYPE AND DATES COVERED
	December 1998	Final, Jan 96 - Jan 98

4. TITLE AND SUBTITLE

Flame Structure Studies of Neat and NH_3-Doped H_2/N_2O/Ar Flames by Laser-Induced Fluorescence, Mass Spectrometry, and Modeling

5. FUNDING NUMBERS

PR: 1L161102AH43

6. AUTHOR(S)

R. C. Sausa and D. T. Venizelos

7. PERFORMING ORGANIZATION NAME(S) AND ADDRESS(ES)

U.S. Army Research Laboratory
ATTN: AMSRL-WM-BD
Aberdeen Proving Ground, MD 21005-5066

8. PERFORMING ORGANIZATION REPORT NUMBER

ARL-TR-1858

9. SPONSORING/MONITORING AGENCY NAMES(S) AND ADDRESS(ES)

10.SPONSORING/MONITORING AGENCY REPORT NUMBER

11. SUPPLEMENTARY NOTES

12a. DISTRIBUTION/AVAILABILITY STATEMENT

Approved for public release; distribution is unlimited.

12b. DISTRIBUTION CODE

13. ABSTRACT *(Maximum 200 words)*

A combined experimental and modeling study of neat and NH_3-doped (Φ = 1), 30-Torr flames is reported. The major species concentrations are measured by molecular beam mass spectrometry (MB/MS), whereas the minor species OH, NH, and O-atom concentrations are measured by laser-induced fluorescence (LIF). The species NO is measured both by LIF and MB/MS, and O_2 by MB/MS. The flame temperatures are measured both by OH and NH LIF and by thin-wire thermometry. The flames are modeled with PREMIX using the temperature profiles and several detailed chemical mechanisms as input. The mechanisms include the ***GRI 2.11***, ***SSLA***, and their derivatives. The ***SSLA*** mechanism was developed previously in our laboratory from a critical literature review. Calculations using all the mechanisms predict fairly well the profiles of the major species for both neat and doped flames. However, both the ***SSLA*** and ***GRI 2.11*** calculations fail to predict the postflame O_2 concentration in the neat flame, the drop in the O_2 concentration with the addition of NH_3, and the NH_3 decay in the doped flame. Sensitivity analyses suggest refinements to the ***SSLA*** and ***GRI 2.11*** mechanisms. The experimental results are predicted rather well using a ***modified SSLA*** mechanism in which the $NH+NO=N_2O+H$ reaction rate is decreased and the $N_2O+M=N_2+O+M$ reaction rate and/or H_2O third-body efficiency is increased to the limit of their uncertainty. Rate analyses performed on the modeled calculations reveal the reactions important to NO, O_2, NH, OH, and O-atom production and consumption and NH_3 consumption. These reactions are presented and discussed.

14. SUBJECT TERMS	15. NUMBER OF PAGES
low-pressure flames, ammonia-doped laser-induced fluorescence, flame-code modeling, mass spectrometry, hydrogen/nitrous oxide	36
	16. PRICE CODE

17. SECURITY CLASSIFICATION OF REPORT	18. SECURITY CLASSIFICATION OF THIS PAGE	19. SECURITY CLASSIFICATION OF ABSTRACT	20. LIMITATION OF ABSTRACT
UNCLASSIFIED	UNCLASSIFIED	UNCLASSIFIED	UL

USER EVALUATION SHEET/CHANGE OF ADDRESS

This Laboratory undertakes a continuing effort to improve the quality of the reports it publishes. Your comments/answers to the items/questions below will aid us in our efforts.

1. ARL Report Number/Author ARL-TR-1858 (Sausa) Date of Report December 1998\

2. Date Report Received _____

3. Does this report satisfy a need? (Comment on purpose, related project, or other area of interest for which the report will be used.) _____

4. Specifically, how is the report being used? (Information source, design data, procedure, source of ideas, etc.) _____

5. Has the information in this report led to any quantitative savings as far as man-hours or dollars saved, operating costs avoided, or efficiencies achieved, etc? If so, please elaborate. _____

6. General Comments. What do you think should be changed to improve future reports? (Indicate changes to organization, technical content, format, etc.) _____

CURRENT ADDRESS

_____
Organization

_____
Name E-mail Name

_____
Street or P.O. Box No.

_____
City, State, Zip Code

7. If indicating a Change of Address or Address Correction, please provide the Current or Correct address above and the Old or Incorrect address below.

OLD ADDRESS

_____
Organization

_____
Name

_____
Street or P.O. Box No.

_____
City, State, Zip Code

(Remove this sheet, fold as indicated, tape closed, and mail.)

(DO NOT STAPLE)